



# Why Does $^1\text{H}$ NMR Signal Intensity of Concentrated Aqueous Acids and Bases Decrease Anomally?

Hanami, Kazuya

Maki, Hideshi

Matsuda, Rei

Mizuhata, Minoru

---

## (Citation)

Electrochemistry, 90(10):103005

## (Issue Date)

2022-10-28

## (Resource Type)

journal article

## (Version)

Version of Record

## (Rights)

© The Author(s) 2022. Published by ECSJ.

This is an open access article distributed under the terms of the Creative Commons Attribution 4.0 License (CC BY), which permits unrestricted reuse of the work in any medium provided the original work is properly cited.

## (URL)

<https://hdl.handle.net/20.500.14094/0100477611>



## The 66th special feature

## "Novel Aspects and Approaches to Experimental Methods for Electrochemistry"

### Why Does $^1\text{H}$ NMR Signal Intensity of Concentrated Aqueous Acids and Bases Decrease Anomalously?


Kazuya HANAMI,<sup>a</sup> Hideshi MAKI,<sup>a,\*</sup> Rei MATSUDA,<sup>b</sup> and Minoru MIZUHATA<sup>a,c,§</sup>
<sup>a</sup> Department of Chemical Science and Engineering, Graduate School of Engineering, Kobe University, 1-1 Rokkodai-cho, Nada-ku, Kobe 657-8501, Japan

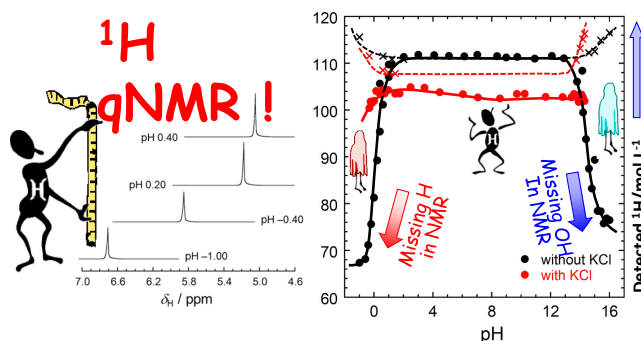
<sup>b</sup> Department of Chemical Science and Engineering, Faculty of Engineering, Kobe University, 1-1 Rokkodai-cho, Nada-ku, Kobe 657-8501, Japan

<sup>c</sup> Faculty of Chemistry, Jagiellonian University, Gronostajowa 2, 30-387 Kraków, Poland

\* Corresponding author: [maki@kobe-u.ac.jp](mailto:maki@kobe-u.ac.jp)

#### ABSTRACT

The signal detection of quantitative  $^1\text{H}$  nuclear magnetic resonance ( $^1\text{H}$  qNMR) for the amount of water in HCl and KOH aqueous solutions at low pH (pH  $\sim 1.2$ ) and high pH (pH 16) was discussed, and an "anomaly of decreasing  $^1\text{H}$  NMR signal intensity" was observed. After adding significant amounts of acid ( $\text{H}^+$ ) or base ( $\text{OH}^-$ ) to the solution for pH regulation, the number of  $^1\text{H}$  nuclei observed by  $^1\text{H}$  NMR significantly decreased at  $\text{pH} \leq 2$  and  $\geq 13$ . The mobility and the activity coefficient of some or all the water molecules hydrated to  $\text{H}_3\text{O}^+$  significantly decreased; hence, they could not be detected by  $^1\text{H}$  qNMR. The remarkably strong electrostatic interactions of the solvent with  $\text{H}_3\text{O}^+$  and  $\text{OH}^-$  significantly reduce the activity coefficient of the solvent by restricting the solvent molecule to the vicinity of the ion. These results are comparable to those reported for vapor pressure measurements and can be attributed to a decrease in activity.  $\text{H}^+$  ( $\text{H}_3\text{O}^+$ ), which has a relatively small ionic radius, has a significant effect on the solvation structure and hydrogen-bond network owing to strong electrostatic interactions with the solvent. Subsequently, significant reduction in the  $^1\text{H}$  NMR relaxation time of the water molecules and signal intensity, along with a low magnetic field shift in the  $^1\text{H}$  NMR signal were also observed in the strongly acidic and strongly basic regions.



© The Author(s) 2022. Published by ECSJ. This is an open access article distributed under the terms of the Creative Commons Attribution 4.0 License (CC BY, <http://creativecommons.org/licenses/by/4.0/>), which permits unrestricted reuse of the work in any medium provided the original work is properly cited. [DOI: 10.5796/electrochemistry.22-66105].




Keywords : Quantitative Nuclear Magnetic Resonance (qNMR), NMR Relaxation, Water Activity, Hydrogen-bond Network

#### 1. Introduction

Information about the interionic interactions and hydration structure in high-concentration electrolyte aqueous solutions is very important from the perspective of expression mechanisms with regard to the physical characteristics of the solutions. This information is particularly useful for concentrated solutions, which are the key in the fields of electrochemistry and molten salt chemistry, and it is necessary to observe the molecular interactions and dynamic behavior of ions and solvent molecules that do not have a sufficient hydration shell in a high-concentration aqueous electrolyte solution. In particular, the physical properties of the solvent, which is the main chemical species in solution, are very important because they affect the equilibrium of the chemical reaction and the behavior of the electrochemical reactions in various solutions. Fourier transform NMR (FT-NMR) spectroscopy is

suitable for detecting solutes and solvent molecules and can be used to observe various solvent properties by measuring the signal intensity, chemical shift, NMR relaxation time, and molecular self-diffusion coefficient. We investigated the hydration structures and interionic interactions of monovalent and divalent metal ions in concentrated aqueous solutions using quantitative NMR (qNMR) measurements. Herein, we report "the anomaly of decreasing  $^1\text{H}$  NMR signal intensity" for water in a high-concentration aqueous electrolyte solution system. This anomaly represents a significant reduction in the  $^1\text{H}$  NMR integrated signal intensity for the water content of the solvent in comparison to its theoretical abundance.<sup>1</sup> In addition, we also found that the decrease in the  $^1\text{H}$  NMR integrated signal intensity was influenced by the ion pair production and concomitant destruction of the stable hydration structure.<sup>1</sup> The relationship between the instrumental constants and intensity for NMR measurements at steady magnetic fields was first reported in 1963, before the widespread use of FT-NMR.<sup>2</sup> Furthermore, with respect to quadrupolar nuclides, the determination of urea, nitrate, and ammonium in aqueous solution using  $^{14}\text{N}$  qNMR was reported by Simeral in 1997.<sup>3</sup> However, since the resolution of the signal

<sup>§</sup>ECSJ Active Member

H. Maki  [orcid.org/0000-0002-8960-4833](https://orcid.org/0000-0002-8960-4833)

M. Mizuhata  [orcid.org/0000-0002-4496-2215](https://orcid.org/0000-0002-4496-2215)

intensity is not very clear when  $^{14}\text{N}$  qNMR is used,  $^1\text{H}$  qNMR is presently becoming a more popular quantitative technique.<sup>4–8</sup> In qNMR, solutes are generally the analysis targets; using solvents as analysis targets for  $^1\text{H}$  qNMR is rare,<sup>9</sup> and only trace amounts of residual solvent in solution can be thus quantified.<sup>10,11</sup> Therefore, the cause of this “anomaly of decreasing  $^1\text{H}$  NMR signal intensity” is mostly unknown, although one likely explanation is that the motility of water molecules in the primary hydration shell of metal ions is significantly reduced.<sup>1</sup> Furthermore, the changes in the activity coefficient of water molecules may be due to the formation of a hydration shell by metal ions or the hydrogen-bond networks in the solution. Although there are many reports on the measurement of electrolyte activity in aqueous electrolyte solutions, the activity data of chemical species in highly concentrated solutions, such as those used in the electrolyte solutions of secondary batteries, and particularly the activity data of the solvent, are not sufficient; thus, further measurements are necessary. These findings are essential for achieving an accurate understanding of the electrochemical reactions that occur in batteries and their efficiencies.

To elucidate the complicated molecular-theoretical phenomena described above that occur in the high-concentration electrolyte solution, an approach to obtain the possible simplest solution is the most effective. Therefore, in this study, “the anomaly of decreasing  $^1\text{H}$  NMR signal intensity” in aqueous HCl or KOH solutions from low pH (i.e., pH  $-1.2$ ) to high pH (i.e., pH 16) was analyzed, and its cause was elucidated via the  $^1\text{H}$  NMR chemical shift and relaxation time. Because HCl and KOH are highly soluble in water, it is possible to conduct analyses over a wide pH range (i.e., extremely high  $\text{H}^+$  ( $\text{H}_3\text{O}^+$ ) and  $\text{OH}^-$  concentrations). In addition,  $\text{H}^+$  ( $\text{H}_3\text{O}^+$ ) and  $\text{OH}^-$ , which have relatively smaller ionic radii, are expected to significantly affect the solvation structure and hydrogen-bond network through strong electrostatic interactions with the solvent. Consequently, a sharp anomaly of decreasing  $^1\text{H}$  NMR signal intensity is observed.

Based on these phenomena, Majima et al. discussed the activity of water in concentrated acid by the vapor pressure measurement of acids when H is present in both, solutes and solvents.<sup>12</sup> Because the measurement is based on interfacial phenomena involving vapor–liquid equilibrium, the concept of active volume in the entire liquid phase, or in bulk, must be introduced.

This study explored the possibility of using qNMR for solvents as an observation probe for ion hydration structures, hydrogen-bond network structures, and solvent activity coefficients in solution. In particular, the activity coefficient of a solvent, a major chemical species in a solution, determines not only the physical properties of the solvent, but also the behavior of the chemical equilibrium and reaction rate. A simple evaluation of the solvent activity coefficient is important for understanding the electrochemical reactions in which the activity coefficient of the chemical species dominates the reaction equilibrium.

## 2. Experimental

### 2.1 Samples

Aqueous sample solutions were prepared from reagent grade HCl, KOH, and KCl (Nacalai Tesque Inc., Japan) and double-distilled water. Two types of acid and base solutions were prepared using the following two methods: In the first method only an acid or base was added to an aqueous solvent. In this case, the as-purchased aqueous HCl or saturated KOH solution was diluted and adjusted to a certain pH range as described below. In the second method an ionic strength,  $1/2\sum c_i z_i^2$ , was adjusted to a concentration of  $1.0\text{ mol L}^{-1}$  by preparing a solution of  $1.0\text{ mol L}^{-1}$  HCl and  $1.0\text{ mol L}^{-1}$  KCl (for acidic region), or  $1.0\text{ mol L}^{-1}$  KOH and  $1.0\text{ mol L}^{-1}$  KCl (for basic region). In this case, the most acidic and basic sample solutions are  $1.0\text{ mol L}^{-1}$  HCl and  $1.0\text{ mol L}^{-1}$  KOH,

respectively. These solutions are indicated as “without KCl” and “with KCl,” respectively.

The pH of the sample solution was measured using a composite glass electrode (9680S-10D; HORIBA Ltd., Japan) connected to a pH/ion meter (F-53; HORIBA Ltd., Japan). The composite glass electrode was calibrated with phthalate, phosphate, and borate buffers at pH 4.02, 6.86, and 9.18, respectively. Although a glass electrode does not guarantee an accurate pH value around 0 or 14 especially, no correction was made to the pH value measured at the glass electrode in order to correlate the “measured”  $\text{H}^+$  activity obtained at the glass electrode with the so-called “activity” of H measured by  $^1\text{H}$  qNMR. The original pH values of the double-distilled water and  $1.0\text{ mol L}^{-1}$  KCl solution are 6.12 and 6.04, respectively. The actual concentration of  $^1\text{H}$  nuclei can be determined from the concentrations of  $\text{H}^+$ ,  $\text{OH}^-$  and water molecules. The concentration of water molecules was determined from the density of the sample solutions and the actual concentrations of  $\text{H}^+$ ,  $\text{OH}^-$ ,  $\text{K}^+$ , and  $\text{Cl}^-$ . The actual  $\text{H}^+$  and  $\text{OH}^-$  concentrations in the sample solution were determined by acid–base titration with oxalic acid as the primary standard.

### 2.2 NMR measurement

$^1\text{H}$  qNMR spectra were recorded on an INOVA 400 (9.39 T) pulse FT–NMR spectrometer (Varian Inc., USA) at  $20.0 \pm 0.5^\circ\text{C}$  using a  $90^\circ$  flip angle single pulse sequence. A coaxial NMR tube system was employed for all  $^1\text{H}$  NMR measurements to avoid the contamination of  $\text{D}_2\text{O}$  for field-frequency locking into the sample solutions.<sup>13</sup> A very short time lag between the pulse irradiation and the FID acquisition start (i.e., dead time) of 5 ms was set. The NMR data acquisition time was 16.0 s, and the digital resolution of the obtained  $^1\text{H}$  NMR spectra was  $1.563 \times 10^{-4}$  ppm. Further extension of the relaxation delay did not change the intensity of the  $^1\text{H}$  NMR spectra. The gain of the RF amplifier in the NMR spectrometer (i.e., receiver gain) was set to a constant value of  $-10\text{ dB}$ . To avoid inaccuracies in the integrated intensities of the  $^1\text{H}$  NMR signals, all  $^1\text{H}$  NMR spectral data after the Fourier transform were carefully corrected for the phase and baseline<sup>5,6,9,13</sup> using the NMR analysis software Mnova ver. 14.2 (Mestrelab Research, S. L., Spain). Lorentzian window function processing for noise reduction was not performed in order to ascertain the quantitative integrity of the NMR output signals. Then, the integrated intensity of all  $^1\text{H}$  NMR signals was calculated manually by the sectional measurement method in Microsoft Excel, with an integral region of ten times the peak width at half height of the signals. The amount of  $^1\text{H}$  nuclei that gave rise to the  $^1\text{H}$  NMR signal was calculated based on the integrated intensity of the  $^1\text{H}$  NMR signal due to pure water (i.e., twice the amount of pure water substance per unit volume,  $55.4 \times 2\text{ mol L}^{-1}$ ) at  $20.0^\circ\text{C}$ .

The  $T_1$  and  $T_2$  of all  $^1\text{H}$  nuclei were determined by the inversion recovery<sup>14</sup> and Carr–Purcell–Meiboom–Gill (CPMG) procedures,<sup>15</sup> respectively, at  $25 \pm 0.5^\circ\text{C}$  without  $\text{D}_2\text{O}$  for field-frequency locking using an Acorn area (magnetic field strength of 0.3 T) as a specialized measuring device for measuring  $^1\text{H}$  NMR relaxation (XiGo Nanotools Inc., USA).

## 3. Results and Discussion

### 3.1 pH dependence of the detected $^1\text{H}$ nuclei amount by NMR

The representative  $^1\text{H}$  NMR spectra observed in this study are shown in Fig. 1. The intensity of the peak attributed to  $^1\text{H}$  nuclei in NMR should depend on the number of H nuclei in the liquid, where added  $\text{H}^+$ , detected as  $\text{H}_3\text{O}^+$ , and  $\text{OH}^-$  in addition to the originally present water are detected with single band due to a significantly faster chemical exchange rate than the time constant of NMR observations. Contrary to this expectation, however, the intensity of the H peak appeared to be smaller in the concentrated acid or base



**Figure 1.** Representative  $^1\text{H}$  NMR spectra of the acid–base solutions without KCl (left) and with KCl (right). The vertical scale shows the measured signal intensity.

regions where H nuclei were added. In addition, the decrease in  $^1\text{H}$  NMR signal intensity and the lower magnetic field shift in  $^1\text{H}$  NMR signals were confirmed in the strongly acidic and basic regions, particularly in the non-supporting electrolyte system.

The amount of  $^1\text{H}$  nuclei detected by NMR and the calculated apparent coefficients,  $\gamma$ , which are regarded as variations of activity corresponding to  $^1\text{H}$  nuclei, are shown in Figs. 2a and 2b, respectively. The intensity of H in the NMR spectra of a certain amount of water should be regarded as the “activity of water to a magnetic field”, and it is interesting to obtain a correlation with pH as an index of the “electrochemical activity” of  $\text{H}^+$ ,  $a_{\text{H}^+}$ . Therefore, to compare both “activity,” the correlation of the NMR intensity of H atoms with pH is shown in Fig. 2. To compare the experimentally obtained values for each, the horizontal axis is the pH value obtained from the glass electrode measurements, independent of the concentration (ionic strength) of the solution of  $\text{H}^+$ . Therefore, because the pH is obtained directly from the glass electrode values, and the ionic strength of the solution is therefore adjusted to  $1 \text{ mol L}^{-1}$  for the system with supporting electrolyte, KCl. However, it is also plotted at values lower than pH 0 or higher than pH 14.

In these figures, the results for the acid and base systems, with and without the  $1.0 \text{ mol L}^{-1}$  KCl as a supporting electrolyte, are included. In the case of “without KCl” the most acidic and basic sample solutions are  $1.0 \text{ mol L}^{-1}$  HCl and  $1.0 \text{ mol L}^{-1}$  KOH, respectively, however their pH is below 0 and above 14 respectively. This is because the glass electrode does not have an ideal Nernstian response in this pH range. For both systems, the amount of detected  $^1\text{H}$  nuclei was almost constant in the pH range between 2 and 13. This suggests a high reproducibility of  $^1\text{H}$  qNMR for solvents. In the case of the non-supporting electrolyte system, little acid or base is added, so the amount detectable by NMR is approximately constant, which is consistent with the deviation in the amount of  $^1\text{H}$  nuclei from  $110.8 \text{ mol L}^{-1}$  in pure water (pointed by solid arrow in Fig. 2a). By contrast, it should be noted that the amount of detected  $^1\text{H}$  nuclei decreases remarkably at pH 2 or lower and also at pH 13 or higher. In the concentrated acidic and basic regions, considerable amounts of acid ( $\text{H}^+$ ) or base ( $\text{OH}^-$ ) were added to the solutions for pH adjustment. As a result, the actual number of  $^1\text{H}$  nuclei in the solutions increased significantly, as shown by the dotted lines containing “x” symbols in Fig. 2a. Notably, the number of  $^1\text{H}$  nuclei detected by NMR was significantly reduced. Therefore, we will now discuss the results in Fig. 2b, which show the ratio of the amount of H calculated from the NMR signal intensity to the actual amount of H, that is, the apparent activity coefficient,  $\gamma$ . The decrease in the number of  $^1\text{H}$  nuclei detected by NMR was accelerated with extreme decreases and increases in pH, and below pH 0 and above pH 15, more than 30 % of the actual abundance of

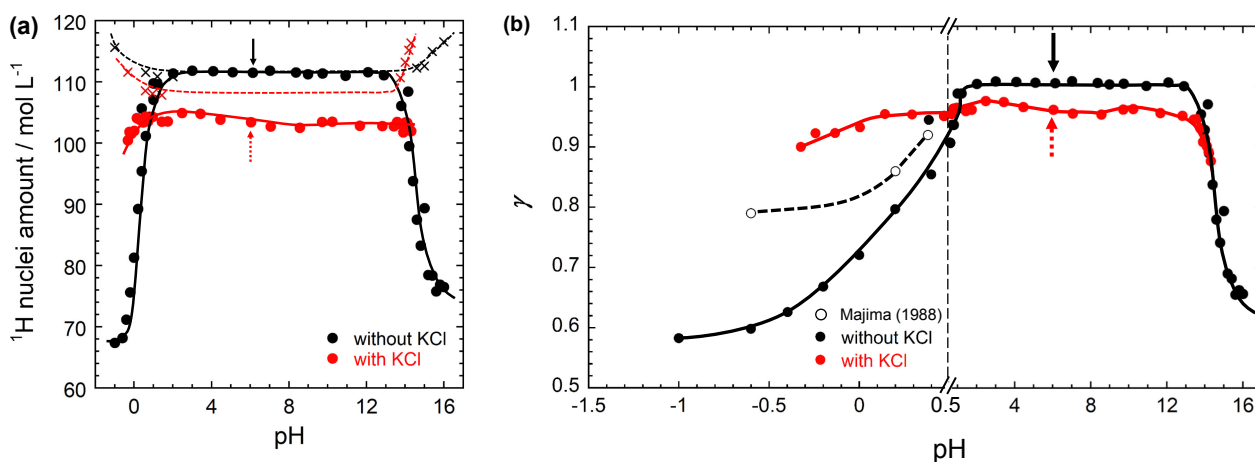


**Figure 2.** pH dependence of (a) the detected  $^1\text{H}$  nuclei amount by  $^1\text{H}$  qNMR and (b) the apparent water activity coefficient calculated from the results of (a). Solid black arrow: pure water without addition of acid or base (pH 6.12). Broken red arrow:  $1.0 \text{ mol L}^{-1}$  KCl without addition of acid or base (pH 6.04). The x-mark and the dotted line in (a) indicate the actual concentration determined by acid–base titration and its variation of  $^1\text{H}$  nuclei in the solution. The open circles in (b) show the  $\gamma$  values for determined by equilibrium for vaporization in Majima’s work.<sup>12</sup>

$^1\text{H}$  nuclei was not detected by  $^1\text{H}$  NMR. Furthermore, the decrease in the number of detected  $^1\text{H}$  nuclei was more remarkable in the strongly acidic region. Even when the supporting electrolyte was included, the amount of detected  $^1\text{H}$  nuclei was originally  $104.9\text{ mol L}^{-1}$  (pointed by broken arrow in Fig. 2a) in the neutral solution whereas the practical amount was  $108.4\text{ mol L}^{-1}$  by the amount of KCl excluded volume. Then, there was a slight increase in the intensity of the detected  $^1\text{H}$  nuclei in the low pH region from neutral pH to pH 2, as well as a decrease in intensity at pH 2 and lower. Additionally, in a system containing KCl, it can be expected that  $\text{K}^+$  which is a structure-disrupting ion disrupts the hydrogen-bonding network and reduces electrostatic interactions with other water molecules. Consequently, the activity of water tends to increase, and in the range of  $\text{pH} < 1$ , the decrease in the activity coefficient is suppressed in the with KCl more than without KCl. Unlike quadrupolar NMR (e.g.,  $^7\text{Li}$ ,  $^{23}\text{Na}$ ,  $^{27}\text{Al}$  NMR, etc.), which is prone to extreme broadening of NMR signals due to the asymmetry of the electric field gradient around a nucleus, and the decrease in molecular mobility, in the case of  $^1\text{H}$  NMR, which is dipolar NMR (e.g.,  $^1\text{H}$ ,  $^{13}\text{C}$ ,  $^{19}\text{F}$  NMR, etc.), the apparent disappearance of the NMR signal is unlikely. Therefore, the decrease in the detected number of  $^1\text{H}$  nuclei in Fig. 2 is considered to be due to the unique cause of dipolar NMR in the uniform phase, which has not been reported to the best of our knowledge. We previously quantified water molecules in high-concentration electrolyte aqueous solutions of alkali metals and alkaline earth metal chlorides by  $^1\text{H}$  qNMR, and found that the amount of water detected by  $^1\text{H}$  qNMR was approximately 10% less than the amount of water that should be detected (i.e., the amount calculated by the density measurement) in the sample solution.<sup>1</sup> Furthermore, the quantitative analysis in the dilute concentration region confirmed that water molecules bound to the primary hydration shell could not be detected by  $^1\text{H}$  NMR because their mobility is extremely limited. It is thought that three water molecules are hydrated to  $\text{H}_3\text{O}^+$ , and they thus exist as  $\text{H}_9\text{O}_4^+$  in aqueous solutions.<sup>16–23</sup> In this study, some or all of the water molecules that hydrated to  $\text{H}_3\text{O}^+$  could not be detected by  $^1\text{H}$  NMR because their mobility was significantly decreased. Moreover, in the strongly basic region, the water molecules in the primary hydration shell of  $\text{OH}^-$ , which significantly increased with the pH adjustment, became undetectable. It can be concluded that the remarkably strong electrostatic interaction of the solvent with  $\text{H}_3\text{O}^+$  and  $\text{OH}^-$ , as described above, significantly reduced the activity of the solvent by restricting the solvent molecule to the vicinity of the ion, thereby decreasing the integrated NMR signal intensity of the solvent molecule. Similarly, electrostatic interactions between the solvent and  $\text{K}^+$  ions also reduce the activity of the solvent. The difference between the dashed and solid lines of “with KCl” in Fig. 2b reflects the decrease in the activity of water hydrated with  $\text{K}^+$  ions.

Single-ion activities of  $\text{H}^+$  and  $\text{Cl}^-$  in relatively dilute HCl aq. below  $1.0\text{ mol kg}^{-1}$  have been reported by Sakaida et al.<sup>24</sup> According to the results of Majima’s experiment, the various activity coefficients of water in the strongly acidic region (i.e.,  $1.0$ – $3.0\text{ mol L}^{-1}$  HCl) decrease with increasing HCl concentration.<sup>12</sup> The determination of water activity by Majima et al. is based on the transpiration method, in which the activity of water molecules as they evaporate near the solid–liquid interface is observed. In contrast, the  $^1\text{H}$  NMR signal intensity of water in this study reflected the activity of water in the liquid phase. These  $\gamma$  values determined by Majima et al.<sup>12</sup> are shown as open circles in Fig. 2b. The  $\gamma$  values obtained in this study can be considered to be consistent with these values. The results by Majima et al. are about  $\gamma = 0.92, 0.86$ , and  $0.79$  (without KCl) at HCl concentrations of  $1.0, 2.0$ , and  $3.0\text{ mol L}^{-1}$ , respectively. Notably, water molecules in different physicochemical environments exhibit similar activity changes. Furthermore, water and hydroxide ions, which are localized around a central water molecule, may affect the structural fluctuations of the

hydrogen-bonding network in aqueous solutions, resulting in the development of specific electrical conductivity. Of course, if such a qNMR method can be used as an indicator of the activity of a particular atom in a solution, it would overcome the difficulty of making accurate vapor pressure measurements that have reached vapor–liquid equilibrium with slight compositional changes and disproportionation.

As described above, we suggest that due to the existence of a “missing molecule for NMR” with regard to the decrease in the mobility of the molecule in the local space in the solution, the physical property information of a specific molecule cannot be obtained by a solution NMR, even in a homogeneous solution. It should also be noted that the observed parameters, such as chemical shift, relaxation time and self-diffusion coefficient by NMR may reflect only the physical properties of “observable” molecules.

### 3.2 pH dependence of $^1\text{H}$ NMR relaxation time

The pH dependence of the spin–lattice relaxation time ( $T_1$ ) and spin–spin relaxation time ( $T_2$ ) of the  $^1\text{H}$  NMR spectra is shown in Fig. 3. All  $T_1$  values are longer than  $T_2$ , in accordance with the theoretical NMR relaxation background. The  $^1\text{H}$  NMR relaxation time also showed a pH dependence similar to that of the integrated signal intensities, as discussed in Section 3.1; namely, both  $T_1$  and  $T_2$  were significantly reduced at pH 0 or lower and pH 14 or higher. The measured relaxation times  $T_1$  and  $T_2$  were calculated from the intensity of the peak based on the response to the magnetic field obtained in the measurement. Therefore, it should be noted that the decrease in relaxation time at the point of sharp decrease in the intensity due to  $^1\text{H}$  nuclei below pH 0 or above pH 15 is not necessarily subject to protons with decreased mobilities that are responsible for the decrease in lost intensity obtained in Section 3.1. Similarly, the observed parameters, such as chemical shift, relaxation time, and self-diffusion coefficient by NMR may reflect only the physical properties of “observable” molecules. Although  $T_1 > T_2$  in the overall pH range, regardless of the presence or absence of KCl, there is no significant difference between them, and  $^1\text{H}$  NMR relaxation is in the “extreme narrowing region.”<sup>25</sup> In the case of a dipole nucleus, such as a  $^1\text{H}$  nucleus, the  $T_1$  and  $T_2$  in the “extreme narrowing region” are approximately expressed by the following equations:<sup>26,27</sup>

$$T_1 = T_2 = \frac{d^6}{10a\gamma^4\tau_c} \quad (1)$$

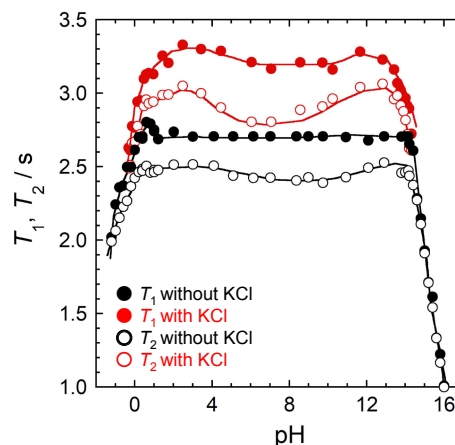


**Figure 3.** pH dependence of the spin–lattice relaxation time ( $T_1$ ) and spin–spin relaxation time ( $T_2$ ) of  $^1\text{H}$  NMR. The  $^1\text{H}$  NMR relaxation time also shows pH dependence in relation to the signal integrated intensities.



where  $a = 3\mu_0^2\hbar^2/320\pi^2$ ,  $\mu_0$  is the vacuum permeability constant,  $d$  is the distance between the nuclei,  $\gamma$  is the gyromagnetic ratio, and  $\tau_c$  is the rotational correlation time of a spherical molecule rotating in a liquid. The reductions in  $T_1$  and  $T_2$  suggest an increase in  $\tau_c$ , that is, a decrease in the rotational mobility of the water molecules. Increasing the  $\text{H}_3\text{O}^+$  and  $\text{OH}^-$  concentrations strengthens the solvate structure and hydrogen-bond network, thereby increasing  $c$  and reducing  $T_1$  and  $T_2$ . The reduction in  $T_1$  and  $T_2$  is more remarkable in the strongly basic region than in the strongly acidic region because of the decrease in the mobility of water molecules associated with an increase in viscosity. However, at the same pH, both  $T_1$  and  $T_2$  of the solution with KCl were longer than those without KCl. This is because the  $\text{K}^+$  ion, which is a structure-breaking ion, destroys the water network structure, resulting in an increase in the mobility of water molecules. As mentioned in the results in Fig. 2b in 3.1, the addition of an acid or base to an electrolyte containing KCl increases the number of hydrogen bonding elements. However, the dynamic properties of individual water molecules experience an increase due to further hydrogen bond scission by the addition of KCl, a structure-breaking ion. Thus, despite adding a small amount of KCl, the maximum values of  $T_1$  and  $T_2$  were observed at pH 3 and 12. The acid and alkali concentrations were only approximately  $10^{-3} \text{ mol L}^{-1}$ , suggesting that the presence of KCl increases the mobility of H elements. A stable hydrogen bond network and ion hydration exist in the neutral region. When the pH was changed to slightly acidic or basic region, the  $\text{H}^+$  and  $\text{OH}^-$  destabilize the hydrogen bond network and hydrated ion, thus, increasing the mobility of water molecules, and as a result, the values of  $T_1$  and  $T_2$  increase. Furthermore, in a strong acid or strong base,  $\text{H}_3\text{O}^+$  and  $\text{OH}^-$  have a strong hydration sphere and the viscosity of the solution increases (especially on the strongly basic side), hence the mobility of water molecules is extremely reduced, and  $T_1$  and  $T_2$  value begins to decrease.

The pH dependence of  $T_2/T_1$ , and the ratio of  $T_1$  to  $T_2$ , is shown in Fig. 4. Notably  $T_2/T_1$  reaches 1 in the strongly acidic and basic regions, regardless of the presence or absence of the supporting electrolyte. This is because the reduction in the  $T_1$  is more remarkable than that in the  $T_2$  in the strongly acidic and basic regions. Spin-lattice relaxation (i.e.,  $T_1$  relaxation) in NMR proceeds by dissipating the Zeeman energy of the nuclear spin system to the phonon system (phonons are quantized lattice vibrations in a medium). Namely, the number of phonons increased due to the strengthening of the hydrogen-bond network in the strongly acidic and basic regions, and the  $T_1$  relaxation of the  $^1\text{H}$  nucleus was accelerated. The intermolecular interactions, such as the solvation structures and the hydrogen-bond networks in the strongly

acidic and basic regions confirmed by  $^1\text{H}$  NMR relaxation time, can cause a reduction in the activities of  $\text{H}_3\text{O}^+$ ,  $\text{OH}^-$ , and  $\text{H}_2\text{O}$ . The reduction in the activity coefficients of these molecules may also contribute to the decrease in the  $^1\text{H}$  NMR signal area intensity.

### 3.3 pH dependence of $^1\text{H}$ NMR chemical shift

Few studies have reported  $^1\text{H}$  NMR chemical shifts of water molecules in concentrated acidic and basic aqueous solutions. Mäemets et al. reported the values of the chemical shift for practical base solutions, such as KOH and NaOH, and calculated the properties of clustered acids and bases without any quantitative analysis.<sup>27</sup> They indicated that in the formation of clusters containing  $\text{H}^+$  or  $\text{OH}^-$  structures in water, both  $\delta(^{17}\text{O})$  and  $\delta(^1\text{H})$  values shift toward lower magnetic fields as the ratio of  $\text{H}^+$  or  $\text{OH}^-$  increases. To confirm the reproducibility of the NMR measurements and analysis, we explored the relationship between chemical shift and signal intensity. Figure 5 shows the pH dependence of the  $^1\text{H}$  NMR chemical shifts observed in the NMR spectra as shown in Fig. 1. From pH 1 to 13, the  $^1\text{H}$  NMR chemical shift was approximately constant, as in the case of the integrated signal intensities and relaxation times. However, the  $^1\text{H}$  NMR signal shifted to a lower magnetic field at pH 1 or lower and pH 13 or higher, and this tendency was stronger in the acidic region than in the basic region, as in the case of the  $^1\text{H}$  NMR signal integrated intensity. This result agrees with that reported by Mäemets et al.<sup>27</sup>  $\text{H}_3\text{O}^+$  is generated by the addition of a  $^1\text{H}$  nucleus (i.e., proton) to  $\text{H}_2\text{O}$ , and the  $^1\text{H}$  nucleus of  $\text{H}_3\text{O}^+$  has a smaller number of electrons per  $^1\text{H}$  nucleus than that of  $\text{H}_2\text{O}$ . Therefore, the  $^1\text{H}$  NMR signal shifted to a lower magnetic field as the  $\text{H}_3\text{O}^+$  concentration increased. This phenomenon is due to a decrease in the magnetic shielding effect. The opposite phenomenon is expected to occur in strongly basic regions, because  $\text{OH}^-$  is generated by the dissociation of protons from  $\text{H}_2\text{O}$ . By simple estimation, the  $^1\text{H}$  nuclei of  $\text{OH}^-$  have more electrons per  $^1\text{H}$  nucleus than those of  $\text{H}_2\text{O}$ ; hence, the  $^1\text{H}$  NMR signal should shift to a higher magnetic field as the  $\text{OH}^-$  concentration increases in response to the increasing magnetic shielding effect. However, a slightly lower magnetic field shift was observed. A possible cause for this low magnetic field shift is the electrostatic interaction between  $\text{K}^+$  and  $\text{OH}^-$ . As a result of the electrostatic interaction between  $\text{K}^+$  and  $\text{OH}^-$ , the  $\text{OH}^-$  has a structure that orients the oxygen atom towards  $\text{K}^+$ ; therefore, the electron cloud around the  $^1\text{H}$  nucleus is attracted in the direction of  $\text{K}^+$  via the oxygen atom. Consequently, the electron density around the  $^1\text{H}$  nucleus was significantly reduced and the  $^1\text{H}$  NMR signal showed a low magnetic field shift as the  $\text{OH}^-$  concentration

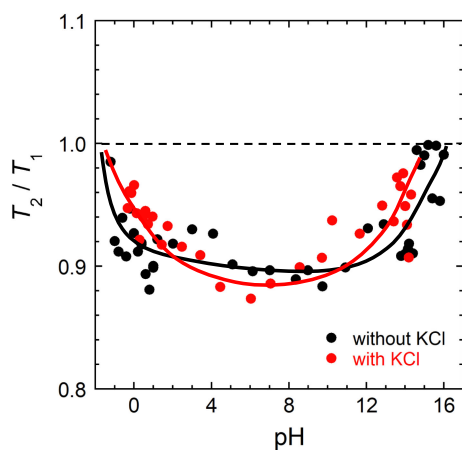


**Figure 4.** pH dependence of  $T_2/T_1$  ratio. The value of  $T_2/T_1$  is asymptotic to 1 in the concentrated acidic and basic regions regardless of the presence or absence of KCl.

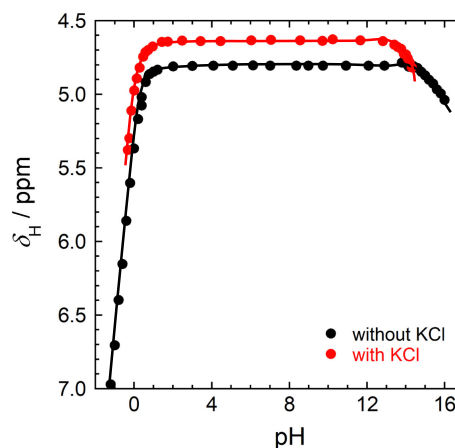


**Figure 5.** pH dependence of the  $^1\text{H}$  NMR chemical shift. The  $^1\text{H}$  NMR signal shifts to a low magnetic field at pH 1 or lower and pH 13 or higher, and this tendency is more remarkable on the acidic region than the basic region.

increased. Notably all or most of the water molecules in the primary hydration shell were not detected by  $^1\text{H}$  NMR, as discussed in Section 3.1. It can be estimated that the  $^1\text{H}$  nucleus responsible for this low magnetic field shift is a water molecule located outside the primary hydration shell. In contrast, in the strongly acidic region a remarkably low magnetic field shift was observed because the electrostatic interactions between  $\text{H}_3\text{O}^+$  and  $\text{Cl}^-$  was very weak. This corresponds to the general fact that the hydration of anions to water is not as pronounced as that of cations. From the above considerations, it is likely that the direction and magnitude of the change in the chemical shift of the  $^1\text{H}$  NMR signal in the strongly acidic and strongly basic regions depend on the type of anion.

#### 4. Conclusions

Here, significant amounts of acid ( $\text{H}^+$ ) or base ( $\text{OH}^-$ ) were added to a solution for pH regulation, and the number of  $^1\text{H}$  nuclei observed by NMR significantly decreased at  $\text{pH} \leq 2$  or  $\geq 13$ . The mobility of some or all the water molecules that hydrated to  $\text{H}_3\text{O}^+$  or  $\text{K}^+$  significantly decreased; hence, the presence of these molecules could not be detected by  $^1\text{H}$  qNMR. Furthermore, the decrease in the number of  $^1\text{H}$  nuclei observed by NMR was more remarkable in the strongly acidic region than in the strongly basic region.  $\text{H}^+$  ( $\text{H}_3\text{O}^+$ ), which has a relatively small ionic radius, not only significantly reduced the mobility of water molecules, owing to its strong electrostatic interaction with the solvent water molecules but also significantly affected the solvation structure and hydrogen bond network. Consequently, a significant decrease in the number of  $^1\text{H}$  nuclei was observed by NMR. The remarkably strong electrostatic interactions of the solvent with  $\text{H}_3\text{O}^+$  and  $\text{OH}^-$  significantly reduced the activity coefficient of the solvent by restricting the solvent molecule to the vicinity of the ion. A significant reduction in the  $^1\text{H}$  NMR relaxation time of the water molecules and a low magnetic field shift in the  $^1\text{H}$  NMR signal were also observed in the strongly acidic and strongly basic regions. The existence of molecules in solution is undetectable by NMR, i.e., “missing molecules for NMR” due to the decrease in the mobility of molecules within the local space of the solution, which was examined in this work, resulted in the inability to obtain the physical property information of a specific molecule by NMR of a homogeneous solution. Notably, the parameters, such as chemical shift, relaxation time, and self-diffusion coefficient, observed in NMR analysis may reflect only the physical properties of the “observable” molecules. Therefore, the results of this work indicate the possibility of using the qNMR analysis of solvents as observation probes for ion hydration structures, hydrogen-bond network structures, and solvent activity coefficients in solution.

#### Acknowledgment

This work was supported by JSPS KAKENHI (Grant-in-Aid for Scientific Research (B)), Grant Number 20H02843.

#### CRedit Authorship Contribution Statement

Kazuya Hanami: Data curation (Lead), Writing – original draft (Equal)  
 Hideshi Maki: Conceptualization (Lead), Data curation (Lead), Funding acquisition (Lead), Methodology (Lead), Project administration (Lead), Writing – original draft (Lead)  
 Rei Matsuda: Data curation (Equal)  
 Minoru Mizuhata: Conceptualization (Equal), Supervision (Lead), Validation (Lead), Writing – review & editing (Lead)

#### Conflict of Interest

The authors declare no conflict of interest in the manuscript.

#### Funding

Japan Society for the Promotion of Science: 20H02843

#### References

- H. Maki, R. Sogawa, M. Fukui, S. Deki, and M. Mizuhata, *Electrochemistry*, **87**, 139 (2019).
- J. L. Jungnickel and J. W. Forbes, *Anal. Chem.*, **35**, 938 (1963).
- L. S. Simeral, *Appl. Spectrosc.*, **51**, 1585 (1997).
- S. K. Bharti and R. Roy, *Trends Anal. Chem.*, **35**, 5 (2012).
- K. Choi, S. Myoung, Y. Seo, and S. Ahn, *Magnetochemistry*, **7**, 15 (2021).
- Y. B. Monakhova and B. W. K. Diehl, *Magn. Reson. Chem.*, **55**, 996 (2017).
- Y. Nishizaki, N. Masumoto, and N. Sugimoto, *Comprehensive Natural Products III* (3rd ed.), Elsevier, Amsterdam, Ch. 7.04 (2020).
- B. Diehl, U. Holzgrabe, Y. Monakhova, and T. Schönberger, *J. Pharm. Biomed. Anal.*, **177**, 112847 (2020).
- H. Maki, M. Takemoto, R. Sogawa, and M. Mizuhata, *Colloids Surf., A*, **562**, 270 (2019).
- R. Muhamadejev, R. Melngaile, P. Paegle, I. Zibarte, M. Petrova, K. Jaudzems, and J. Veliks, *J. Org. Chem.*, **86**, 3890 (2021).
- E. Kang, H. R. Park, J. Yoon, H. Yu, S. Chang, B. Kim, K. Choi, and S. Ahn, *Microchem. J.*, **138**, 395 (2018).
- H. Majima, E. Peters, Y. Awakura, S. K. Park, and M. Aoki, *Metall. Trans., B*, **19**, 53 (1988).
- H. Maki, T. Tachibana, S. J. Eun, and M. Mizuhata, *Colloids Surf., A*, **604**, 125286 (2020).
- R. L. Vold, J. S. Waugh, M. P. Klein, and D. E. Phelps, *J. Chem. Phys.*, **48**, 3831 (1968).
- S. Meiboom and D. Gill, *Rev. Sci. Instrum.*, **29**, 688 (1958).
- C. T. Wolke, J. A. Fournier, L. C. Dzugas, M. R. Fagiani, T. T. Odbadrakh, H. Knorke, K. D. Jordan, A. B. McCoy, K. R. Asmis, and M. A. Johnson, *Science*, **354**, 1131 (2016).
- R. Grahn, *Ark. Fys.*, **1**, 13 (1962).
- T. K. Esser, H. Knorke, and K. R. Asmis, *J. Phys. Chem. Lett.*, **9**, 798 (2018).
- M. R. Fagiani, H. Knorke, T. K. Esser, N. Heine, C. T. Wolke, S. Gewinner, W. Schöllkopf, M.-P. Gaigeot, R. Spezia, M. A. Johnson, and K. R. Asmis, *Phys. Chem. Chem. Phys.*, **18**, 26743 (2016).
- J. M. Headrick, E. G. Diken, R. S. Walters, N. I. Hammer, R. A. Christie, J. Cui, E. M. Myshakin, M. A. Duncan, M. A. Johnson, and K. D. Jordan, *Science*, **308**, 1765 (2005).
- K. Yagi and B. Thomsen, *J. Phys. Chem. A*, **121**, 2386 (2017).
- H. Wang and N. Agmon, *J. Phys. Chem. A*, **121**, 3056 (2017).
- Q. Yu and J. M. Bowman, *J. Chem. Phys.*, **146**, 121102 (2017).
- H. Sakaida and T. Kakiuchi, *J. Phys. Chem. B*, **115**, 13222 (2011).
- J. W. Akitt, *NMR and Chemistry: An Introduction to Modern NMR Spectroscopy* (3rd ed.), Chapman & Hall, London, Chapter 4.2 (1992).
- I. Solomon, *Phys. Rev.*, **99**, 559 (1955).
- V. Mäemets and I. Koppel, *J. Chem. Soc., Faraday Trans.*, **93**, 1539 (1997).